



Laser-induced dynamic alignment and nonlinear-like optical transmission in liquid suspensions of 2D atomically thin nanomaterials

QIUHUI ZHANG,^{1,10} YANAN WANG,^{2,3,4,10,11}  FENG LIN,^{2,3} YINGJIE TANG,⁵ PEIHONG CHENG,⁶ XUFENG ZHOU,⁷ ZHUAN ZHU,³ YAYAO MA,⁸ ZHAOPING LIU,⁷ DONG LIU,⁵ LAICHEN LIU,² CHENGZHEN QIN,² ZHONGCHEN CHEN,² ZHIMING WANG,^{2,12} AND JIMING BAO^{3,9,13} 

¹Department of Electrical Information Engineering, Henan University of Engineering, Xinzheng, Henan 451191, China

²Institute of Fundamental and Frontier Sciences, University of Electronic Science and Technology of China, Chengdu, Sichuan 610054, China

³Department of Electrical and Computer Engineering, University of Houston, Houston, Texas 77204, USA

⁴Currently with the Department of Electrical and Computer Engineering, University of Nebraska-Lincoln, Lincoln, Nebraska 68588, USA

⁵Department of Mechanical Engineering, University of Houston, Houston, Texas 77204, USA

⁶School of Electronic and Information Engineering, Ningbo University of Technology, Ningbo, Zhejiang 315211, China

⁷Key Laboratory of Graphene Technologies and Applications of Zhejiang Province, Ningbo Institute of Materials Technology and Engineering, Chinese Academy of Sciences, Ningbo, Zhejiang 315201, China

⁸School of Optical and Electronic Information, Huazhong University of Science and Technology, Wuhan, Hubei 430074, China

⁹Department of Physics and Texas Center for Superconductivity, University of Houston, Houston, Texas 77204, USA

¹⁰These authors contributed equally to this paper.

¹¹yanan.wang@unl.edu

¹²zhmwang@uestc.edu.cn

¹³jbao@uh.edu

Abstract: Nonlinear optical property of atomically thin materials suspended in liquid has attracted a lot of attention recently due to the rapid development of liquid exfoliation methods. Here we report laser-induced dynamic orientational alignment and nonlinear-like optical response of the suspensions as a result of their intrinsic anisotropic properties and thermal convection of solvents. Graphene and graphene oxide suspensions are used as examples, and the transition to ordered states from initial optically isotropic suspensions is revealed by birefringence imaging. Computational fluid dynamics is performed to simulate the velocity evolution of convection flow and understand alignment-induced birefringence patterns. The optical transmission of these suspensions exhibits nonlinear-like saturable or reverse saturable absorptions in Z-scan measurements with both nanosecond and continuous-wave lasers. Our findings not only demonstrate a non-contact controlling of macroscopic orientation and collective optical properties of nanomaterial suspensions by laser but also pave the way for further explorations of optical properties and novel device applications of low-dimensional nanomaterials.

© 2021 Optical Society of America under the terms of the [OSA Open Access Publishing Agreement](https://doi.org/10.1364/OE.440062)

1. Introduction

The interaction of light with low-dimensional nanomaterials has attracted enormous research interest in order to understand their unique electronic and optical properties for the subsequent development of novel optoelectronic devices. Atomically thin two-dimensional (2D) nanomaterials have emerged as novel optoelectronic materials with intrinsic anisotropic and nonlinear optical properties [1–5]. Due to the development of exfoliation method, most 2D materials can be conveniently obtained in a large quantity in liquid suspension [6,7]. Compared with dry solid samples, a liquid suspension of 2D materials in a cuvette is easy to handle and suffers less optical damages. Thus, most reported studies of nonlinear optical properties of 2D materials are carried out in their liquid suspensions [5,8–32]. However, the effect of solvent on the optical measurements still has not been paid enough attention [5,8–32].

Nonlinear optical property of a material allows people to control light with light [5]; however, high peak intensity is required to induce a huge change to its optical constant [4,5], which limits its wide applications. An alternative approach is to use light to induce structural or orientation change of constituent molecules or nanostructures of a material. This approach has been realized in liquid crystals, and there have been growing interests in using light to control many other properties of liquid crystals besides optical property [33–35]. 2D flakes possess large geometric anisotropy and their liquid suspensions can exhibit typical features as liquid crystals [36]. By changing the orientation of individual 2D platelets, the optical property can be changed, and this has been demonstrated by electric or magnetic fields [37–39]. However, unlike conventional liquid crystals, it is still a challenge to use light to change their orientation despite some reports in the literature.

Previously, we pointed out that the claimed coherent self-modulation of the transmitted laser beam is actually a thermal lens effect from solvent [16], and the so-called nonlinear optical limiting is due to strong scattering from laser-induced bubbles [40]. Thus, they have little to do with $\chi^{(3)}$ nonlinear susceptibility of 2D materials. In this work, we report a general phenomenon in the liquid suspension of anisotropic nanomaterials: laser-induced self-alignment and the associated dynamic optical response. Liquid suspensions of graphene and graphene oxide flakes are used to illustrate this laser-induced dynamic alignment, which is revealed by a birefringence imaging technique. Computational fluid dynamics is performed to understand the coupled dynamics of temperature, flow, and suspended 2D materials. This phenomenon is a result of the complicated interaction of laser with a composite fluid. By performing polarization-dependent Z-scan measurements, the influence of laser-induced alignment on nonlinear-like optical transmission has also been revealed. The understanding of self-alignment and dynamic responses is essential to further exploring and understanding the intrinsic optical properties of nanomaterials as well as their applications in optical manipulation and optical switching.

2. Materials and experimental setup

Materials and experimental setup are similar to those in our previous work [16]. Few-layer graphene flakes with a lateral dimension of a few micrometers are synthesized via intercalation and exfoliation of natural graphite. Single-layer graphene oxide (GO) flakes with sizes in the range of 2~10 μm are prepared by a modified Hummers' method [6,16]. As-obtained graphene and graphene flakes are dispersed in N-methyl-2-pyrrolidone (NMP) by sonication and form stable suspensions with a concentration of 0.005–0.01% in weight percentage (wt%), corresponds to 0.002–0.004% in volume fraction (vol%).

Figure 1(a) shows the experimental setup for the birefringence imaging, which is a hybrid combination between a Z-scan measurement and a typical birefringence imaging system. A 532-nm continuous-wave (CW) laser is focused into a 10-mm cuvette filled with suspension by a 100 mm lens (spot size of 80 μm). A collimated white light (halogen lamp) shares the same path

with the CW laser by a 50:50 beamsplitter, which is used to capture the birefringence images accompanied by a pair of polarizers and a camera. A 532-nm long-pass filter is put behind the cuvette to eliminate the disturbance of 532-nm CW laser. Optical transmission behaviors of the suspension have been investigated by a traditional Z-scan setup, employing either a CW laser at 532 nm or 150 nanoseconds (ns) laser pulses (1 kHz repetition rate) at 527 nm. But a cube polarizing beamsplitter is put in front of the lens to control the polarization direction of

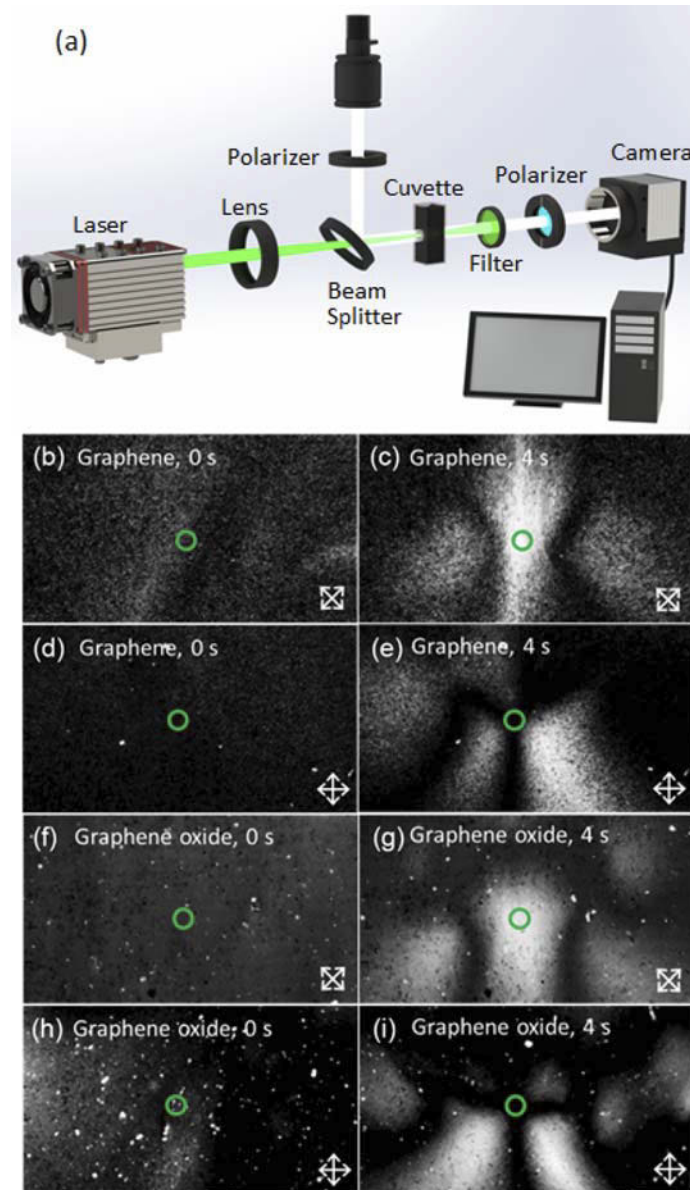


Fig. 1. Birefringence imaging (see Visualization 1). (a) Schematic of birefringence imaging experimental setup. Snapshots of birefringence images of (b-e) graphene and (f-i) GO suspensions in NMP. Arrows indicate the directions of polarizer/analyzer. Laser power: 20 mW, horizontally polarized. Green circles indicate the laser spots with $\sim 80 \mu\text{m}$ in diameter. The sparkles and dark spots come from thicker flakes.

the laser (horizontally or vertically polarized); thereby, the effect of laser polarization on the optical transmission of suspension can be explored. The transmitted laser power is monitored by a photodiode power meter with computer control and readout.

3. Results and discussion

The anisotropy of 2D nanomaterials is an important distinction compared to the near isotropy of many other light absorbers such as dye molecules. This property allows us to probe the orientation and dynamics of flakes. Figures 1(b)–(i) show birefringence images of liquid suspensions of graphene and GO before and after CW laser illumination. Initial dark images through two crossed-polarizers indicate that flakes are randomly orientated due to their low concentration [37,41]. As the laser is turned on, clear convection movements can be observed in the suspensions, and stable birefringence patterns gradually form after 4 seconds (see Visualization 1). Based on the birefringence images between two crossed-polarizers, we can figure out the orientations of graphene shown in Fig. 2(a), where the flake directors are perpendicular to the laser propagation direction inside the laser spot. Note that even after the birefringence patterns become stable, the suspensions remain in motion constantly. The stable birefringence patterns have little dependence on the laser polarization (Supplement 1, Fig. S1). After turning off the laser, the convection and birefringence of suspensions slowly disappear, and the crossed-polarization images resume uniformly dark.

Such orientation is also confirmed by measuring the polarization dependent transmission of the laser beam itself as shown in Fig. 2(b). The polarization dependent absorption is due to the shape and optical anisotropy of graphene or GO flakes; the absorption is larger when the laser polarization is parallel to the plane of graphene [37,41]. It is important to point out that the initial suspension is optically isotropic because of low concentrations of graphene and GO; the appearance of nematic phase and birefringence is another indication of their strong optical anisotropy. The birefringence images clearly show that the alignment is not limited to the flakes located inside the laser beam. The power and polarization-dependent transmission in Fig. 2(b) also reveals that the alignment is strongly correlated to the laser power; the difference in transmission between two polarizations diminishes as the laser power is reduced. These observations suggest that the flake alignment is induced by the convection flow of the carrier fluid, not the electrical field of the laser, as speculated in some previous reports [42,43].

To better understand the alignment process of the 2D flakes, we compute the temperature distribution and the flow field using computational fluid dynamics (CFD) [16]. Due to the dilute concentration of graphene, its effect on the thermophysical properties of the solvent, such as density, thermal conductivity, specific heat capacity, and viscosity, is negligible. The heat transfer from graphene to the surrounding liquid after the optical absorption is considered instantaneous due to the extremely small thermal mass of the graphene flakes. Figure 3 illustrates the corresponding velocity fields, where there is barely any flow at 0.4 seconds, but increases considerably at 4 seconds. The driving force here is the viscous shear force from the surrounding fluid medium. A flake will experience an imbalance in shear forces on its head and tail ends, resulting in a net torque that causes the flake to rotate. In fact, the orientations of graphene flakes shown in the schematic of Fig. 2(a) agree well with the streamline in the same region in Fig. 3(b), further demonstrating a good correlation between the laser-induced convection flow and the dynamic alignment of flakes.

Because the above liquid convection is driven by a laser's photothermal energy, a pulsed laser beam can also induce similar flow and alignment as long as its repetition frequency is greater than 10 Hz, which is satisfied by nearly all the lasers used in Z-scan and nonlinear optics [5,11–14,16,22,25,30,31]. Moreover, the flow-induced alignment is not limited to 2D nanomaterials [21], but universal to low-dimensional nanomaterials with large geometric anisotropy, such as one-dimensional (1D) carbon nanotubes [43] or nanowires [44]. Although

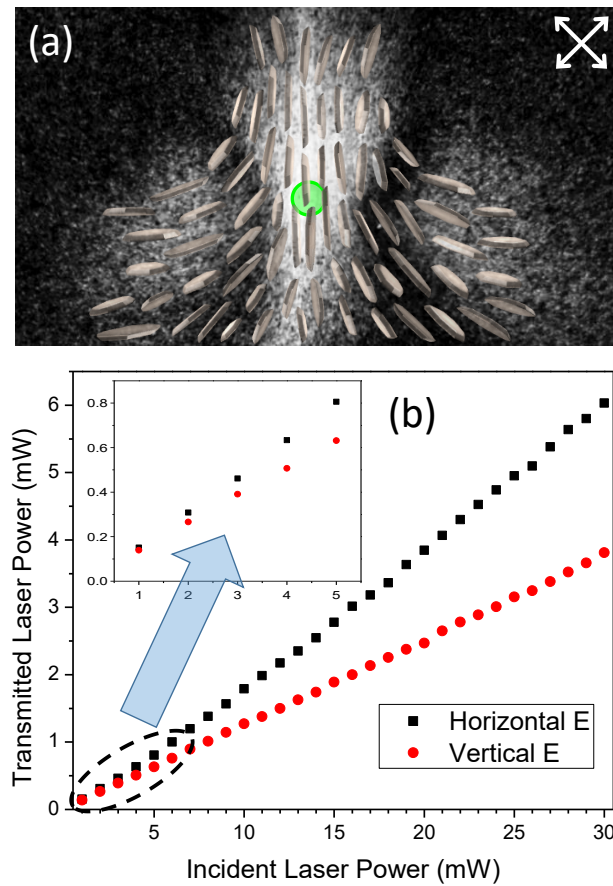


Fig. 2. Flow-induced alignment and the consequential influence on optical transmission. (a) Schematic of orientations of graphene flakes in NMP suspension based on the birefringence images. Green circles indicate the laser spots. (b) Transmitted laser power (P_T) as a function of laser polarization and incident power (P_I) in the same liquid suspension of graphene in (a). The suspension is placed at the focus point of the 532-nm CW laser.

the flow-induced alignment of graphene and other nanostructures has been achieved by applying mechanical forces [43–46], laser beams enable non-contact and more precise control to manipulate individual nanostructures and suspensions. It should be noted that thermophoresis or the Soret effect was proposed to explain nonlinear absorption in GO suspension [47], but a direct observation of GO thermophoresis was not provided. Although thermophoresis is driven by temperature gradient, it is only important at very low flow velocities [48]. As such, thermophoresis can be neglected in that case as well as in our experiments where large convection flows are generated by lasers. In fact, our videos have clearly shown that suspended nanostructures are moving along the flow patterns rather than temperature gradients [49,50]. We also want to point out that temperature gradient is dependent on many thermophysical properties of a solvent such as thermal conductivity and viscosity. For example, water has a higher thermal conductivity than NMP. Our previous work showed that temperature gradient in water was significantly reduced, but the flow velocity remained high, as can be seen from the distorted diffraction ring pattern [51]. Thus, laser-induced alignment is a common phenomenon in suspended nanostructures even confined in a small volume [51].

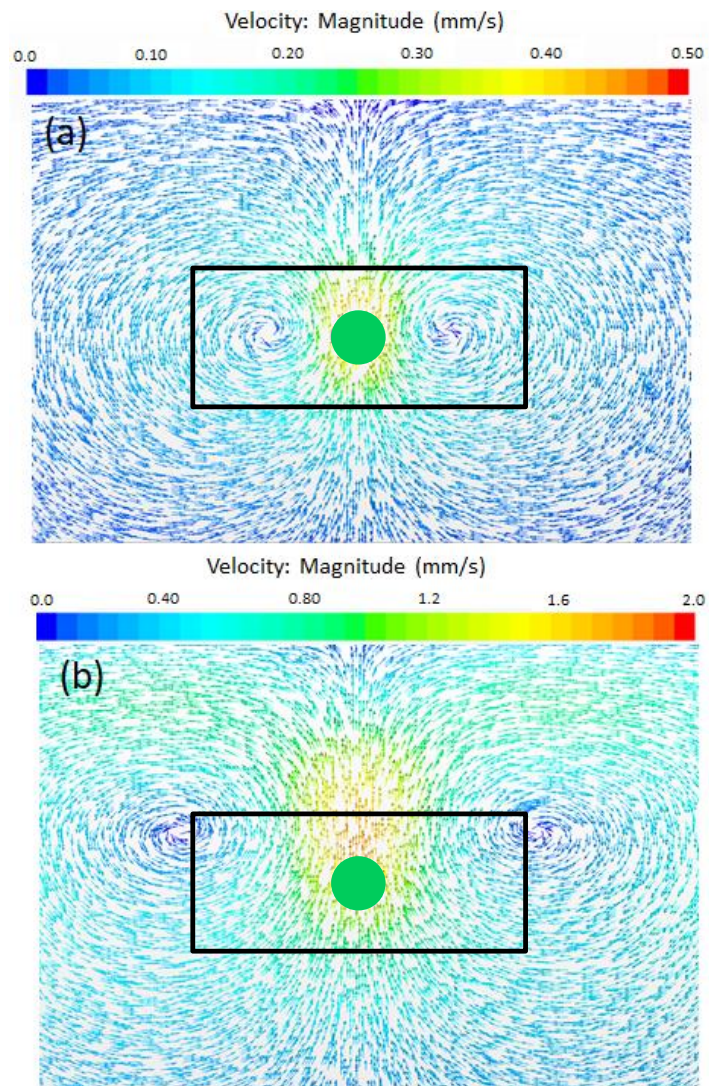


Fig. 3. Simulation of the flow velocity distribution of graphene in NMP. The illumination time at (a) 0.4 seconds and (b) 4.0 seconds. Green dots indicate the laser spots. The black rectangle in (b) corresponds to the region of the birefringence image in Fig. 2(a).

Another important finding of this work is the modulation in optical transmission arising from the aligned flakes and their optical anisotropy. As preliminarily shown in Fig. 2(b), the suspensions transform from optically isotropic to nematic phase due to the laser-induced alignment and exhibit birefringence and polarization-dependent transmission to the incident laser. To further explore this self-modulating behavior, we performed open-aperture Z-scan measurements in graphene and GO suspensions with 532-nm CW laser and 527-nm ns laser pulses. It can be expected when the suspension is out of the focus, the laser-induced temperature gradient and subsequent fluid flow are relatively weak; the flow and subsequent alignment will be much stronger when a focused beam passes through the suspension, as shown in Fig. 1. Because the flakes within the laser path will be aligned vertically, an enhanced optical transmission for horizontally polarized beam but a reduced transmission for vertically polarized laser should be witnessed in the Z-scan experiment. For CW laser excitation, Figs. 4(a) and 4(b) clearly show such Z-scan curves for both graphene and GO suspensions: saturable absorption-like (SA-like) curve for horizontally polarized beam but optical limiting-like (OL-like) curve for vertical polarization at the same incident laser power. Note that the change of transmission in Figs. 4(a) and 4(b) is larger for horizontally polarized light. This is because of much smaller optical absorption when the field is perpendicular to the flake planes compared to that parallel to the flakes, similar to the transmission experiments in mechanically aligned GO flakes [37,41]. Such polarization-dependent transmission behaviors have been validated by applying an out-of-focus nanosecond pulsed laser with similar photon energy as well (Figs. 4(c)–4(d)). However, the pulsed laser with a significantly large power density compared to the CW laser induces intense microbubbles and consequential scattering effects when the suspension is placed around the focus point, giving rise to sizeable dips in the transmission curves regardless of laser polarization [36].

The polarization-dependent optical transmission of nanosecond laser was also studied and shown in Fig. 5(b). In comparison, the normalized transmission of CW laser is plotted in Fig. 5(a) based on the same data from Fig. 2(b). As discussed above, in the CW regime, for the horizontally polarized beam, the transmission increases with the incident laser power, while for vertically polarized light, the transmission is reduced. In the nanosecond regime, a similar difference is observed between two polarizations; but unlike CW laser, nanosecond pulses with both polarizations begin to exhibit OL-like rapid drop in transmission at about 10 mW [40]. The importance of self-alignment and polarization is clear, and we are now in a good position to discuss many of previous Z-scan and transmission experiments, especially for the ones excited by nanosecond pulsed lasers and CW lasers. Note that nonlinear-like transmission can also be observed in close-aperture Z-scan experiment, which is typically used to measure the real part of nonlinear refractive index n_2 [52]. As shown in Fig. S2 in Supplement 1, at a low power of 7 mW, a characteristic transmission curve is observed [53]. However, the Z-scan transmission develops into a broad dip at higher laser powers. These features can be understood through the thermal lens effect. At high laser power, a large diffraction ring pattern will appear, leaving behind much weaker transmitted light in the center of the laser beam.

Since most nonlinear optical studies of 2D materials suspended in solution do not consider the effect of fluid convection and the induced alignment, it is not accurate to simply ascribe the observed nonlinear-like transmissions to their intrinsic nonlinear property, no matter whether the experiments are performed with femtosecond [12–14], picosecond [9,12,22,31], nanosecond [5,8–12,15–17,23–26,30,31], or CW lasers [18–20,27–29,32], and no matter whether the nano-materials are 1D carbon nanotubes (CNTs) [10,17,23,27,28], graphene [5,9–11,15,26], graphene oxide [8–10,12,18,26,31,32], transition metal dichalcogenides (TMDCs) [16,22,24] or black phosphor [13,14,25,30]. For example, as the most common experimental configuration, many observed nonlinear-like Z-scan curves, SA-like enhanced transmission [13,14,22,25,29,30], OL-like reduced transmission [15,17,18,20–24,26–28], or the transition from SA to OL [8,9,12,16,24,30,31],

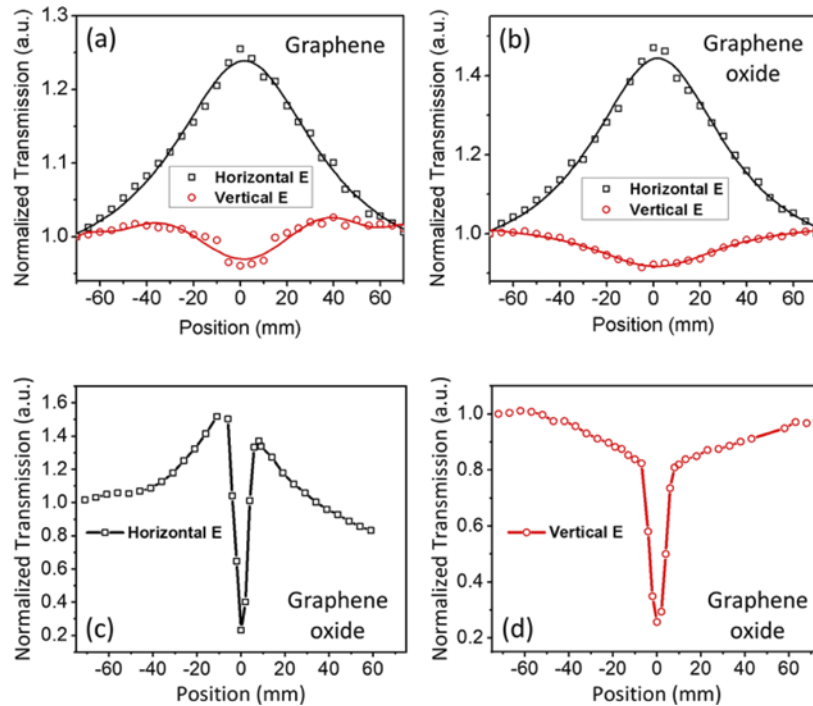


Fig. 4. Open-aperture Z-scan measurements. Z-scan curves of (a) graphene and (b) GO suspensions in NMP under 532-nm CW laser. (c) and (d) are Z-scan curves of GO suspension in NMP under 527-nm ns laser pulses. The measurements are performed by translating the cuvette along the laser beam axis (from far to close) through the focus with a linear motorized stage. The Z-scan curves are obtained by normalizing the transmitted laser power with the value measured far from the focus point. The power of the CW laser is 30 mW, and the focal length is 150 mm. The average power of ns laser pulses is 100 mW, and the focal length is 100 mm.

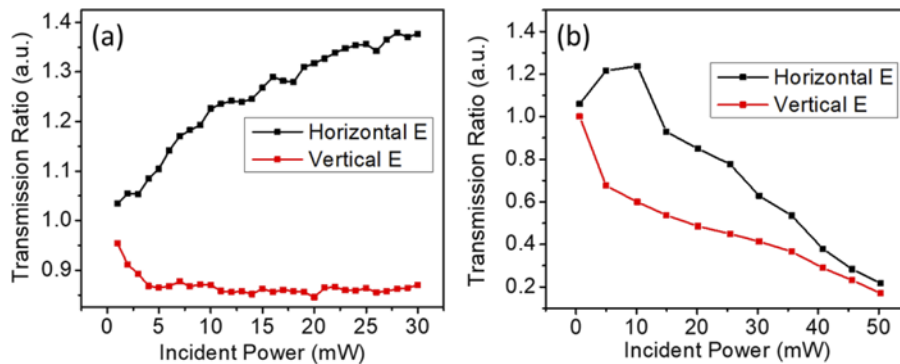


Fig. 5. Power-dependent transmission measurements. Polarization-dependent nonlinear-like optical transmission through graphene suspension under (a) 532-nm CW laser and (b) 527-nm ns laser pulses. The laser is focused into suspension, and then the energy of the incident laser is increased gradually. The transmission ratios are calculated as the ratios between optical transmissions measured at various incident laser power and the one measured at near-zero power. The CW transmission in (a) is based on data from Fig. 2(b). The suspension is placed at the focus point of the lasers.

could be due to a combined effect of laser polarization and flow-induced alignment, as described above.

Another criteria to determine whether the observed nonlinear-like transmissions come from the intrinsic third-order susceptibilities $\chi^{(3)}$ is the laser pulse width. As discussed before [16], sub-picosecond laser pulses with a high peak intensity are required to meet the timescale of electronic transitions [54–56]. The peak intensity of CW lasers and most nanosecond pulses are too low to induce a significant nonlinear optical effect despite the observations of obvious nonlinear-like Z-scan transmissions. It should be pointed out that even with sub-picosecond laser pulses, it is hard to avoid the thermal lens effect and bubble scattering [57,58].

4. Conclusions

In summary, birefringence imaging and CFD reveal that graphene and GO flakes are dynamically aligned by laser heating induced convection flow. Suspended nanostructures absorb the incident laser energy and convert it into heat. The heat is then transferred to the surrounding liquid, creating a local temperature gradient and natural convection, which in turn aligns shape-anisotropic nanostructures with the flow stream. Laser-induced dynamic alignment and optical anisotropy of nanomaterials further result in polarization-dependent modulation of laser transmission. Saturable absorption-like (SA-like) and optical limiting-like (OL-like) transmission has been observed under both continuous-wave and nanosecond pulsed lasers, which should not be misinterpreted as third-order nonlinear effects from electronic or dielectric polarization of nanomaterials. An accurate understanding of 2D atomically thin nanomaterials, solvent fluids, as well as their interactions with laser beam provides valuable guidelines to design optical transmission measurements to explore nonlinear optical properties of nanomaterial suspensions. Moreover, laser-induced dynamic alignment can lead to novel applications of 2D nanomaterials in photonics and optofluidics.

Funding. National Science Foundation (EEC-1530753); Welch Foundation (E-1728); National Natural Science Foundation of China (52002049, 61805071, 62075034, U2004162); China Postdoctoral Science Foundation (2015M582535); Fundamental Research Funds for the Central Universities (ZYGX2015J135).

Disclosures. The authors declare no conflict of interest.

Data availability. Data underlying the results presented in this paper are not publicly available at this time but may be obtained from the authors upon reasonable request.

Supplemental document. See [Supplement 1](#) for supporting content.

References

1. F. Bonaccorso, Z. Sun, T. Hasan, and A. C. Ferrari, “Graphene photonics and optoelectronics,” *Nat. Photonics* **4**(9), 611–622 (2010).
2. A. K. Geim and K. S. Novoselov, “The rise of graphene,” *Nat. Mater.* **6**(3), 183–191 (2007).
3. J. B. Khurgin, “Graphene-A rather ordinary nonlinear optical material,” *Appl. Phys. Lett.* **104**(16), 161116 (2014).
4. B. A. Ruzicka, L. K. Werake, H. Zhao, S. Wang, and K. P. Loh, “Femtosecond pump-probe studies of reduced graphene oxide thin films,” *Appl. Phys. Lett.* **96**(17), 173106 (2010).
5. L. Yan, Y. Xiong, J. Si, X. Sun, W. Yi, and X. Hou, “Optical limiting properties and mechanisms of single-layer graphene dispersions in heavy-atom solvents,” *Opt. Express* **22**(26), 31836–31841 (2014).
6. X. Zhou and Z. Liu, “A scalable, solution-phase processing route to graphene oxide and graphene ultralarge sheets,” *Chem. Comm.* **46**, 2611–2613 (2010).
7. K. Parvez, Z.-S. Wu, R. Li, X. Liu, R. Graf, X. Feng, and K. Mullen, “Exfoliation of graphite into graphene in aqueous solutions of inorganic salts,” *J. Am. Chem. Soc.* **136**(16), 6083–6091 (2014).
8. N. Liaros, K. Iliopoulos, M. M. Stylianakis, E. Koudoumas, and S. Couris, “Optical limiting action of few layered graphene oxide dispersed in different solvents,” *Opt. Mater.* **36**(1), 112–117 (2013).
9. Z. B. Liu, Y. Wang, X. L. Zhang, Y. F. Xu, Y. S. Chen, and J. G. Tian, “Nonlinear optical properties of graphene oxide in nanosecond and picosecond regimes,” *Appl. Phys. Lett.* **94**(2), 021902 (2009).
10. M. Feng, H. B. Zhan, and Y. Chen, “Nonlinear optical and optical limiting properties of graphene families,” *Appl. Phys. Lett.* **96**(3), 033107 (2010).

11. G. K. Lim, Z. L. Chen, J. Clark, R. G. S. Goh, W. H. Ng, H. W. Tan, R. H. Friend, P. K. H. Ho, and L. L. Chua, "Giant broadband nonlinear optical absorption response in dispersed graphene single sheets," *Nat. Photonics* **5**(9), 554–560 (2011).
12. X.-L. Zhang, Z.-B. Liu, X.-C. Li, Q. Ma, X.-D. Chen, J.-G. Tian, Y.-F. Xu, and Y.-S. Chen, "Transient thermal effect, nonlinear refraction and nonlinear absorption properties of graphene oxide sheets in dispersion," *Opt. Express* **21**(6), 7511–7520 (2013).
13. K. P. Wang, B. M. Szydłowska, G. Z. Wang, X. Y. Zhang, J. J. Wang, J. J. Magan, L. Zhang, J. N. Coleman, J. Wang, and W. J. Blau, "Ultrafast Nonlinear Excitation Dynamics of Black Phosphorus Nanosheets from Visible to Mid-Infrared," *ACS Nano* **10**(7), 6923–6932 (2016).
14. S. B. Lu, L. L. Miao, Z. N. Guo, X. Qi, C. J. Zhao, H. Zhang, S. C. Wen, D. Y. Tang, and D. Y. Fan, "Broadband nonlinear optical response in multi-layer black phosphorus: an emerging infrared and mid-infrared optical material," *Opt. Express* **23**(9), 11183–11194 (2015).
15. X. Cheng, N. Dong, B. Li, X. Zhang, S. Zhang, J. Jiao, W. J. Blau, L. Zhang, and J. Wang, "Controllable broadband nonlinear optical response of graphene dispersions by tuning vacuum pressure," *Opt. Express* **21**(14), 16486–16493 (2013).
16. N. Dong, Y. Li, S. Zhang, X. Zhang, and J. Wang, "Optically Induced Transparency and Extinction in Dispersed MoS₂, MoSe₂, and Graphene Nanosheets," *Opt. Mater.* **5**(19), 1700543 (2017).
17. L. Vivien, P. Lancon, D. Riehl, F. Hache, and E. Anglaret, "Carbon nanotubes for optical limiting," *Carbon* **40**(10), 1789–1797 (2002).
18. F. Ghasemi, S. Razi, and K. Madanipour, "Single-step laser-assisted graphene oxide reduction and nonlinear optical properties exploration via CW laser excitation," *J. Electron. Mater.* **47**(5), 2871–2879 (2018).
19. M. A. Pirlar, M. R. Mirghaed, Y. Honarmand, S. M. S. Movahed, and R. Karimzadeh, "Light scattering through the graphene oxide liquid crystal in a micro-channel," *Opt. Express* **27**(17), 23864–23874 (2019).
20. S. Changaei, J. Zamir-Anvari, N.-S. Heydari, S. G. Zamharir, M. Arshadi, B. Bahrami, J. Rouhi, and R. Karimzadeh, "The Large and Tunable Nonlinear Absorption Response of Graphene Oxide Liquid Crystals," *J. Electron. Mater.* **48**(10), 6216–6221 (2019).
21. M. R. Mirghaed, M. A. Pirlar, M. M. Jahanbakhshian, and R. Karimzadeh, "Microfluidic tuning of linear and nonlinear absorption in graphene oxide liquid crystals," *Opt. Lett.* **46**(2), 206–209 (2021).
22. K. Zhou, M. Zhao, M. Chang, Q. Wang, X. Wu, Y. Song, and H. Zhang, "Size-dependent nonlinear optical properties of atomically thin transition metal dichalcogenide nanosheets," *Small* **11**(6), 694–701 (2015).
23. R. Y. Krivenkov, T. N. Mogileva, K. G. Mikheev, A. V. Okotrub, and G. M. Mikheev, "Heat-induced dip of optical limiting threshold in carbon nanotube aqueous suspension," *J. Phys. Chem. C* **122**(28), 16339–16345 (2018).
24. N. N. Dong, Y. X. Li, Y. Y. Feng, S. F. Zhang, X. Y. Zhang, C. X. Chang, J. T. Fan, L. Zhang, and J. Wang, "Optical Limiting and Theoretical Modelling of Layered Transition Metal Dichalcogenide Nanosheets," *Sci. Rep.* **5**(1), 14646 (2015).
25. L. Gao, J. Xu, Z. Zhu, C. Hu, L. Zhang, Q. Wang, and H. Zhang, "Small molecule-assisted fabrication of black phosphorus quantum dots with a broadband nonlinear optical response," *Nanoscale Res. Lett.* **8**(33), 15132–15136 (2016).
26. Y. F. Xu, Z. B. Liu, X. L. Zhang, Y. Wang, J. G. Tian, Y. Huang, Y. F. Ma, X. Y. Zhang, and Y. S. Chen, "A Graphene Hybrid Material Covalently Functionalized with Porphyrin: Synthesis and Optical Limiting Property," *Adv. Mater.* **21**(12), 1275–1279 (2009).
27. M. D. Zidan, A. W. Allaf, M. B. Alsous, and A. Allahham, "Investigation of optical nonlinearity and diffraction ring patterns of carbon nanotubes," *Opt. Laser Technol.* **58**, 128–134 (2014).
28. M. H. M. Ara, H. Akheratdoost, and E. Koushki, "Self-diffraction and high nonlinear optical properties of carbon nanotubes under CW and pulsed laser illumination," *J. Mol. Liq.* **206**, 4–9 (2015).
29. E. Koushki, M. Esmaili, S. A. J. Mohammadi, and P. W. De Oliveira, "Enhancing optical re-orientation effect using external electric field in aluminum-doped zinc oxide nanocolloids," *J. Opt. Soc. Am. B* **36**(8), 2148–2153 (2019).
30. J. Huang, N. Dong, S. Zhang, Z. Sun, W. Zhang, and J. Wang, "Nonlinear absorption induced transparency and optical limiting of black phosphorus nanosheets," *ACS Photonics* **4**(12), 3063–3070 (2017).
31. N. Liaros, P. Aloukos, A. Kolokithas-Ntoukas, A. Bakandritsos, T. Szabo, R. Zboril, and S. Couris, "Nonlinear Optical Properties and Broadband Optical Power Limiting Action of Graphene Oxide Colloids," *J. Phys. Chem. C* **117**(13), 6842–6850 (2013).
32. I. Parra, S. Valbuena, and F. Racedo, "Measurement of non-linear optical properties in graphene oxide using the Z-scan technique," *Spectrochim. Acta A Mol. Biomol. Spectrosc.* **244**, 118833 (2021).
33. K. Ichimura, S. Furumi, S. y. Morino, M. Kidowaki, M. Nakagawa, M. Ogawa, and Y. Nishiura, "Photocontrolled orientation of discotic liquid crystals," *Adv. Mater.* **12**(13), 950–953 (2000).
34. S.-T. Sun, W. M. Gibbons, and P. J. Shannon, "Alignment of guest-host liquid crystals with polarized laser light," *Liq. Cryst.* **12**(5), 869–874 (1992).
35. C. Xue, J. Xiang, H. Nemati, H. K. Bisoyi, K. Gutierrez-Cuevas, L. Wang, M. Gao, S. Zhou, D.-k. Yang, O. D. Lavrentovich, A. Urbas, and Q. Li, "Light-driven reversible alignment switching of liquid crystals enabled by azo thiol grafted gold nanoparticles," *ChemPhysChem* **16**(9), 1852–1856 (2015).
36. F. Lin, X. Tong, Y. Wang, J. Bao, and Z. M. Wang, "Graphene oxide liquid crystals: synthesis, phase transition, rheological property, and applications in optoelectronics and display," *Nanoscale Res. Lett.* **10**(1), 1–16 (2015).

37. F. Lin, Z. Zhu, X. Zhou, W. Qiu, C. Niu, J. Hu, K. Dahal, Y. Wang, Z. Zhao, Z. Ren, D. Litvinov, Z. Liu, Z. M., Wang, and J. M. Bao, "Orientation Control of Graphene Flakes by Magnetic Field: Broad Device Applications of Macroscopically Aligned Graphene," *Adv. Mater.* **29**(1), 1604453 (2017).
38. T. Z. Shen, S. H. Hong, and J. K. Song, "Electro-optical switching of graphene oxide liquid crystals with an extremely large Kerr coefficient," *Nat. Mater.* **13**(4), 394–399 (2014).
39. D. Rossi, J. H. Han, W. Jung, J. Cheon, and D. H. Son, "Orientational Control of Colloidal 2D-Layered Transition Metal Dichalcogenide Nanodiscs via Unusual Electrokinetic Response," *ACS Nano* **9**(8), 8037–8043 (2015).
40. Q. H. Zhang, Y. Qiu, F. Lin, C. Niu, X. F. Zhou, Z. P. Liu, M. K. Alam, D. S. Y., W. Zhang, J. Hu, Z. Wang, and J. M. Bao, "Photoacoustic identification of laser-induced microbubbles as light scattering centers for optical limiting in a liquid suspension of graphene nanosheets," *Nanoscale* **12**(13), 7109–7115 (2020).
41. L. Q. He, J. Ye, M. Shuai, Z. Zhu, X. F. Zhou, Y. A. Wang, Y. Li, Z. H. Su, H. Y. Zhang, Y. Chen, Z. P. Liu, Z. D. Cheng, and J. M. Bao, "Graphene oxide liquid crystals for reflective displays without polarizing optics," *Nanoscale* **7**(5), 1616–1622 (2015).
42. Y. Wu, Q. Wu, F. Sun, C. Cheng, S. Meng, and J. Zhao, "Emergence of electron coherence and two-color all-optical switching in MoS₂ based on spatial self-phase modulation," *Proc. Natl. Acad. Sci. U.S.A.* **112**(38), 11800–11805 (2015).
43. X. W. He, W. L. Gao, L. J. Xie, B. Li, Q. Zhang, S. D. Lei, J. M. Robinson, E. H. Haroz, S. K. Doorn, W. P. Wang, R. Vajtai, P. M. Ajayan, W. W. Adams, R. H. Hauge, and J. Kono, "Wafer-scale monodomain films of spontaneously aligned single-walled carbon nanotubes," *Nature Nanotech.* **11**(7), 633–638 (2016).
44. G. Yu, A. Cao, and C. M. Lieber, "Large-area blown bubble films of aligned nanowires and carbon nanotubes," *Nature Nanotech.* **2**(6), 372–377 (2007).
45. Z. Xu and C. Gao, "Graphene in Macroscopic Order: Liquid Crystals and Wet-Spun Fibers," *Acc. Chem. Res.* **47**(4), 1267–1276 (2014).
46. Y. Huang, X. Duan, Q. Wei, and C. M. Lieber, "Directed assembly of one-dimensional nanostructures into functional networks," *Science* **291**(5504), 630–633 (2001).
47. R. Prizia, C. Conti, and N. Ghofraniha, "Soret reverse saturable absorption of graphene oxide and its application in random lasers," *J. Opt. Soc. Am. B* **36**(1), 19–25 (2019).
48. E. E. Michaelides, "Brownian movement and thermophoresis of nanoparticles in liquids," *Int. J. Heat Mass Tran.* **81**, 179–187 (2015).
49. Y. Wang, Q. Zhang, Z. Zhu, F. Lin, J. Deng, G. Ku, S. Dong, S. Song, M. K. Alam, D. Liu, Z. Wang, and J. Bao, "Laser streaming: Turning a laser beam into a flow of liquid," *Sci. Adv.* **3**(9), e1700555 (2017).
50. S. Yue, F. Lin, Q. Zhang, N. Epie, S. Dong, X. Shan, D. Liu, W. K. Chu, Z. Wang, and J. Bao, "Gold-implanted plasmonic quartz plate as a launch pad for laser-driven photoacoustic microfluidic pumps," *Proc. Natl. Acad. Sci. U. S. A.* **116**(14), 6580–6585 (2019).
51. Y. Wang, Y. Tang, P. Cheng, X. Zhou, Z. Zhu, Z. Liu, D. Liu, Z. M. Wang, and J. M. Bao, "Distinguishing Thermal Lens Effect from Electronic Third-order Nonlinear Self-phase Modulation in Liquid Suspensions of 2D Nanomaterials," *Nanoscale* **9**(10), 3547–3554 (2017).
52. P. B. Chapple, J. Staromlynska, J. A. Hermann, T. J. McKay, and R. G. McDuff, "Single-beam Z-scan: Measurement techniques and analysis," *J. Nonlinear Opt. Phys.* **06**(03), 251–293 (1997).
53. N. Karamitsos, D. Kyrginas, and S. Couris, "On the measurement of the nonlinear optical response of graphene dispersions using fs lasers," *Opt. Lett.* **45**(7), 1814–1817 (2020).
54. M. G. Kuzyk, R. A. Norwood, J. W. Wu, and A. F. Garito, "Frequency dependence of the optical Kerr effect and third-order electronic nonlinear-optical processes of organic liquids," *J. Opt. Soc. Am. B* **6**(2), 154–164 (1989).
55. E. Hendry, P. J. Hale, J. Moger, A. K. Savchenko, and S. A. Mikhailov, "Coherent nonlinear optical response of graphene," *Phys. Rev. Lett.* **105**(9), 097401 (2010).
56. R. R. Alfano, L. L. Hope, and S. L. Shapiro, "Electronic mechanism for production of self-phase modulation," *Phys. Rev. A* **6**(1), 433–438 (1972).
57. M. Maillard, M.-P. Pileni, S. Link, and M. A. El-Sayed, "Picosecond self-induced thermal lensing from colloidal silver nanodisks," *J. Phys. Chem. B* **108**(17), 5230–5234 (2004).
58. C. H. R. Ooi and A. I. Sanny, "Multispectral sparkling of microbubbles with a focused femtosecond laser," *J. Opt. Soc. Am. B* **34**(10), 2072–2080 (2017).